Bulletin of Engineering Geology and the Environment (2020) 79:4933–4946
https://doi.org/10.1007/s10064-020-01852-5

ORIGINAL PAPER

Evaluation of size reduction process for rock aggregates in cone crusher

Ekin Köken [1]

Received: 26 February 2019 / Accepted: 20 May 2020 / Published online: 4 June 2020

Abstract

The size reduction process of rocks in cone crushers is one of the most important issues, particularly for the secondary and tertiary stages of crushing operations. In this study, 17 different rock types were considered for the evaluation of their size reduction variations that occurred in a laboratory-scale cone crusher. Based on several mineralogical, physico-mechanical, and aggregate properties determined for each rock type, the crushability tests were performed.

Before and after the crushability tests, particle size distribution (PSD) of the uncrushed (feed) and crushed (product) materials were determined by sieve analyses. On the basis of these PSDs, the degree of rock crushability (DRC) was attempted to quantify by simple approaches (i.e., size reduction ratio, SRR, and the theoretical square mesh aperture size that corresponds to the 10% of the cumulative undersize in the product, P_{10} (mm)).

The crushability test results demonstrated that the DRC in cone crusher could be quantified by focusing on the variations in the SRR and P_{10}. The SRR and P_{10} are associated with three important rock properties, Shore hardness (SH), Los Angeles abrasion loss (LAA, %), and Brazilian tensile strength (BTS, MPa). The textural and mineralogical features of rocks also have substantial impacts on the DRC for several rock types. It was concluded that the combination of the SRR and P_{10} could be considered together for the evaluation of DRC in cone crushers. Moreover, further research potentials on the DRC were also discussed in this study.

Keywords Crushed rock · Aggregate · Size reduction · Cone crusher · Rock crushability

Introduction

The size reduction process of rocks plays a vital role in the quantity of desired product size with optimum energy consumption. The degree of rock crushability (DRC) has recently become a fascinated research area in terms of economic efficiency, sustainability, and the productivity of rock quarrying. In the mining industry, the size reduction processes of rocks are mainly accomplished by gyratory, impactors (i.e., horizontal and vertical shaft impactors), jaw, and cone crushers in the primary, secondary, and tertiary crushing operations. Some of these crushers have been investigated to clarify several issues such as the crushing mechanism, energy consumption, reducing fines during the crushing action, and wear rate estimations (Guimaraes et al. 2007; Mitchell et al. 2008; Korman et al. 2015, and Terva et al. 2018). In a jaw crusher, for instance, the crushing action occurs as a result of compression, indirect tensile, and impact forces. Rock aggregates are broken down under compression forces induced by the throw of moving jaw. The evaluation of size reduction lasts by the generation of finer materials due to contact loading of jaw plates, smashing of aggregates as well as the inter-particle compression (Fig. 1a). The size reduction process in a cone crusher, on the other hand, evolves like a series of crushing events. It simply occurs by the rotation of the cone mantle that squeezes rocks with different sizes between the cone mantle and concave chamber. The cone mantle rotates on the axis of main shaft with an eccentric motion, and it approaches the concave chamber at the same time during its rotation. In this way, rocks are broken down and discharge the crusher by gravity (Fig. 1b).

The crushability, grindability, and cutability of rocks are associated with many factors. During the size reduction processes in a jaw crusher and rod mill, crushing and grinding

✉ Ekin Köken
ekin.koken@agu.edu.tr

[1] Department of Materials Science and Nanotechnology Engineering, Abdullah Gül University, 38100 Kayseri, Turkey

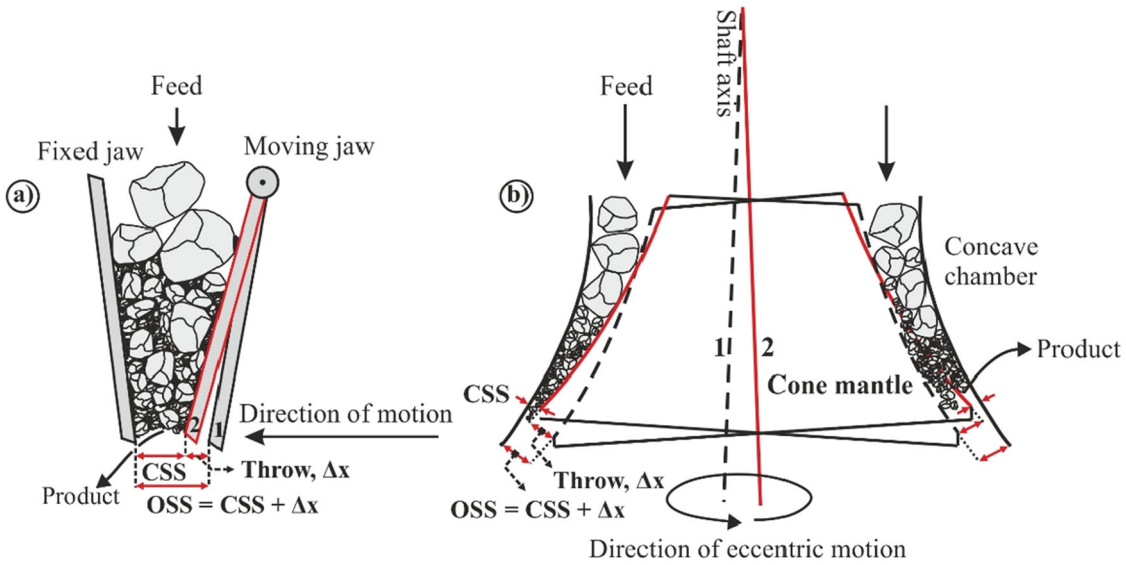

Fig. 1 Schematic representations of rock fracturing in several crushers. **a** Jaw crusher. **b** Cone crusher (modified after Kelly and Spottiswood 1982 and Lee and Evertsson 2011)

energy consumption increase when finer size fractions of the product are desired (Zeng and Forssberg 1992). Heikkilä (Heikkila 1991) reported that the lithological features affect the attrition typology of rocks in primary crushing processes. Donovan (2003) found remarkable relationships between the specific energy consumption and several mechanical rock properties such as deformation modulus and fracture toughness for the assessment of rock comminution by jaw crusher.

The texture and mineralogical composition of rocks are significant variables that control their crushing resistance (Kekec et al. 2006). Olaleye (2010) stated that increasing rock strength properties causes longer crushing times in jaw crusher. Gent et al. (2012) demonstrated that the grinding resistance of brittle minerals increases with increasing their Vickers hardness. Textural properties of rocks also have a significant influence on the specific energy consumption during rock cutability (Öztürk et al. 2004). Yılmaz (2011) concluded that increasing the Vickers and Rosiwal hardness of rocks leads to increasing the specific wear rate of the stonecutter. Mwanga et al. (2015) reviewed the applicability of several testing methods to evaluate the size reduction rate of ores for geometallurgical processes. The researchers pointed out that several testing methods such as mineral hardness and ore/rock strength (e.g., uniaxial compressive strength (UCS, MPa), Brazilian tensile strength (BTS, MPa)) could be considered in geometallurgical size reduction processes owing to their simplicity and repeatability.

The DRC has mainly investigated by using jaw and cone crushers rather than other crusher types. Excluding lithological variances and strength properties of rocks, the DRC in jaw crusher is closely dependent upon several operational factors such as the distance of jaw plates (i.e., open-side discharge setting, OSS, and closed-side discharge setting, CSS), aggregate size, the speed of moving jaw plate, wear condition of jaw plates, and the quantity of the feed (Kahraman et al. 2018). The DRC in jaw crusher was attempted to quantify by several researchers (Kahraman and Toraman 2008; Toraman et al. 2010; Kahraman et al. 2018; Comakli and Cayirli 2019). In these studies, the DRC was quantified as a crushability index (CI, %), which was determined based on sieve analyses of the crushed particles passing through various sieves. The researchers mentioned above showed that the CI related to jaw crushers could be correlated with Los Angeles abrasion loss (LAA, %), impact strength index (ISI, %), UCS, and the BTS of rocks as well.

Similarly, Köken and Özarslan (2018) come up with a new term, compressive crushing value (CCV), whose testing methodology has several modifications of the CI testing procedure proposed by Kahraman et al. (2018). Accordingly, strong correlations were obtained between the CCV and various rock and aggregate properties such as the UCS, aggregate impact value (AIV, %), and the S_{20} brittleness index, whereby lower CCV values represent higher crushing resistance of rock aggregates. Based on these studies concerning the rock crushability, it is clear that jaw crushers were more commonly utilized for the assessment of the DRC. The results obtained from the crushability tests related to jaw crushers could provide a piece of practical knowledge about the crushing resistance rate of rocks since jaw crushers are mainly located below the rock-feeding hopper in most crushing—screening plants. Therefore, further efforts are needed for jaw crushers relating to production yield and product flakiness.

Cone crushers noted for their ability to crush hard, abrasive ores, and rocks are of prime importance in the secondary and

tertiary stages of crushing operations. The size reduction process in cone crushers was mainly focused on considering crushing operational factors rather than rock properties. Regarding the product-based evaluations, Eloranta (1995) showed that the PSD of feeding materials and the CSS play a significant role in the product flakiness in cone crushers. Evertsson (1998) and Quist and Evertsson (2016) established that the variations in the eccentric speed of the cone mantle affect the particle size distribution (PSD) of products. For the assessment of product flakiness in cone crushing, Bengtsson and Evertsson (2006) established an empirical formula as functions of the CSS and average feed size. Lee and Evertsson (2011) stated that increasing the CSS of the cone crusher results in obtaining various production yield rates for specific size fractions. Ma et al. (2016) showed that the variations in the PSD of feeding material have influences on the wear rate of the cone crusher liners. Apart from the operational factors affecting the DRC in cone crushers, Bearman et al. (1997) concluded that the crushing energy consumption in cone crusher is associated with the tensile strength of rocks.

Although product-based evaluations in cone crushing have been documented by the above-mentioned studies, it seems that the DRC in cone crushers from engineering geological aspects has been neither considered nor published previously. Therefore, it seems logical to suppose that the DRC in cone crushers should be investigated in more detail, considering possible effecting factors on rock comminution during cone crushing.

The scope of the present study is to investigate the variations in the DRC that occurred in a laboratory-scale cone crusher for different rock lithologies. For this purpose, several mineralogical, physico-mechanical, and aggregate properties of 17 rock types were determined. The crushability tests were performed using rock aggregates with a particle size range of 11.2–16 mm. Before and after crushability tests, initial and final PSD of rock aggregates were determined by sieve analyses. Based on these PSDs, the DRC was quantified by simple approaches for each rock type. Given crushability test results as a sign of the DRC were then compared with the mineralogical, physico-mechanical, and aggregate properties of the rocks.

Materials and methods

Representative rock samples were obtained from various quarries located in Turkey, and a total of 17 different rock types were used within the scope of this study. Sampling locations and descriptive codes of each rock type are listed in Table 1. The experimental studies were divided into three parts. In the first part, the mineralogical characterization of the rocks was determined by thin-section analyses. In the second part, physico-mechanical properties of rocks such as dry density (ρ_d, g/cm^3), water absorption by weight (w_a, %), Shore hardness (SH), UCS, and BTS were determined in accordance with the suggested methods by the International Society of Rock Mechanics (ISRM 2007).

Table 1 Sampling location and descriptive codes of the rocks investigated

Rock type	Location	Mentioned code
Gabbro	Yenice/Karabük	R_1
Granodiorite	Havran/Balıkesir	R_2
Granite	Küre/Kastamonu	R_3
Basalt	Işıkkara/Kütahya	R_4
Basaltic andesite	Ereğli/Zonguldak	R_5
Andesite	Havran/Balıkesir	R_6
Andesite	Gökçebey/Zonguldak	R_7
Diabase	Ulus/Bartın	R_8
Trachy andesite	Alaplı/Zonguldak	R_9
Gneiss	Güney/Denizli	R_{10}
Fine–grained sandstone	Üzülmez/Zonguldak	R_{11}
Medium–grained sandstone	Amasra/Bartın	R_{12}
Coarse–grained sandstone	Azdavay/Kastamonu	R_{13}
Limestone	Incivez/Zonguldak	R_{14}
Limestone	Eflani/Karabük	R_{15}
Limestone	Havran/Balıkesir	R_{16}
Limestone	Çaycuma/Zonguldak	R_{17}

The mechanical aggregate properties considered in this study were the brittleness index (S_{20}, %) and Los Angeles abrasion loss (LAA, %) that were determined in accordance with the methodologies described by Dahl et al. (2012) and TS EN 1097–2 (2010), respectively.

In the third part of the laboratory studies, the crushability tests were performed using a laboratory–scale cone crusher. The technical properties of the cone crusher and operational factors during the tests are listed in Table 2.

Table 2 Technical properties of the cone crusher and operational factors during crushability tests

Technical properties		Operational factors	
Nominal voltage (V)	380	OSS (mm)	18
Nominal power (kW)	3.0	CSS (mm)	8
Frequency (Hz)	50	Eccentric throw (mm)	10
Feeding gape (mm)	≤ 30	Eccentric speed (rpm)	700
Maximum feed size (mm)	≤ 25		
Feeding capacity (kg/h)	≤ 100		
Power factor	0.90		

OSS open-side discharge setting, *CSS* closed-side discharge setting

The cone mantle was connected to a three-phase AC motor with several worm gear kits and vee-belt pulleys. The length of the cone mantle was approximately 40 cm, and the curve angle of the concave chamber was 23° from top to bottom.

Laboratory studies

Mineralogical characterization of the rocks

Using a polarized microscope, the rocks were characterized from a mineralogical point of view. For this purpose, thin sections were prepared for each rock type, and the quantities of rock-forming minerals were determined using these thin sections. Typical thin sections of the rocks are shown in Fig. 2. According to thin section observations, investigated rocks were divided into three different groups with respect to their lithologies. Igneous rocks were gabbro, granodiorites, granite, basalt, basaltic andesite, andesite, trachy-andesite, and diabase. Sedimentary rocks were sandstones with varying grain sizes and limestones with different textural features. The only metamorphic rock in this study was gneiss.

The mineralogical composition of each rock type is listed in Table 3. Accordingly, igneous rocks are mainly composed of quartz, orthoclase, plagioclase, pyroxene (both orthopyroxene and clinopyroxene), olivine, hornblende, and opaque minerals (i.e., hematite, magnetite, rutile, etc.) with different quantities.

The gabbros (R_1) have a poikilitic texture; equant and small prismatic grains mainly enclose phneocrystals. The granites and granodiorites (R_{2-3}) are granular and phaneritic in texture. The andesitic rocks (R_{5-7}, R_9) have a wide range of textures that vary from aphanitic to porphyritic types. Some of the andesites (e.g., R_6) have weathering signs such as sericitization, chloritization, and argillization in such cases. The basalts (R_4) have a hyalopilitic texture; granular minerals are observed as floating in the groundmass (volcanic matrix).

The diabases (R_8) are in an ophitic texture, and lath-shaped plagioclases were found to be intruded into pyroxenes in thin-section analyses. The gneisses (R_{10}) have a wide range of mineral assemblages (i.e., containing quartz, orthoclase, plagioclase, biotite, muscovite, chlorite, and opaque minerals). They have a granoblastic texture, and rock-forming minerals were observed as foliated fabrics in thin sections. The sandstones (R_{11-13}) are mainly

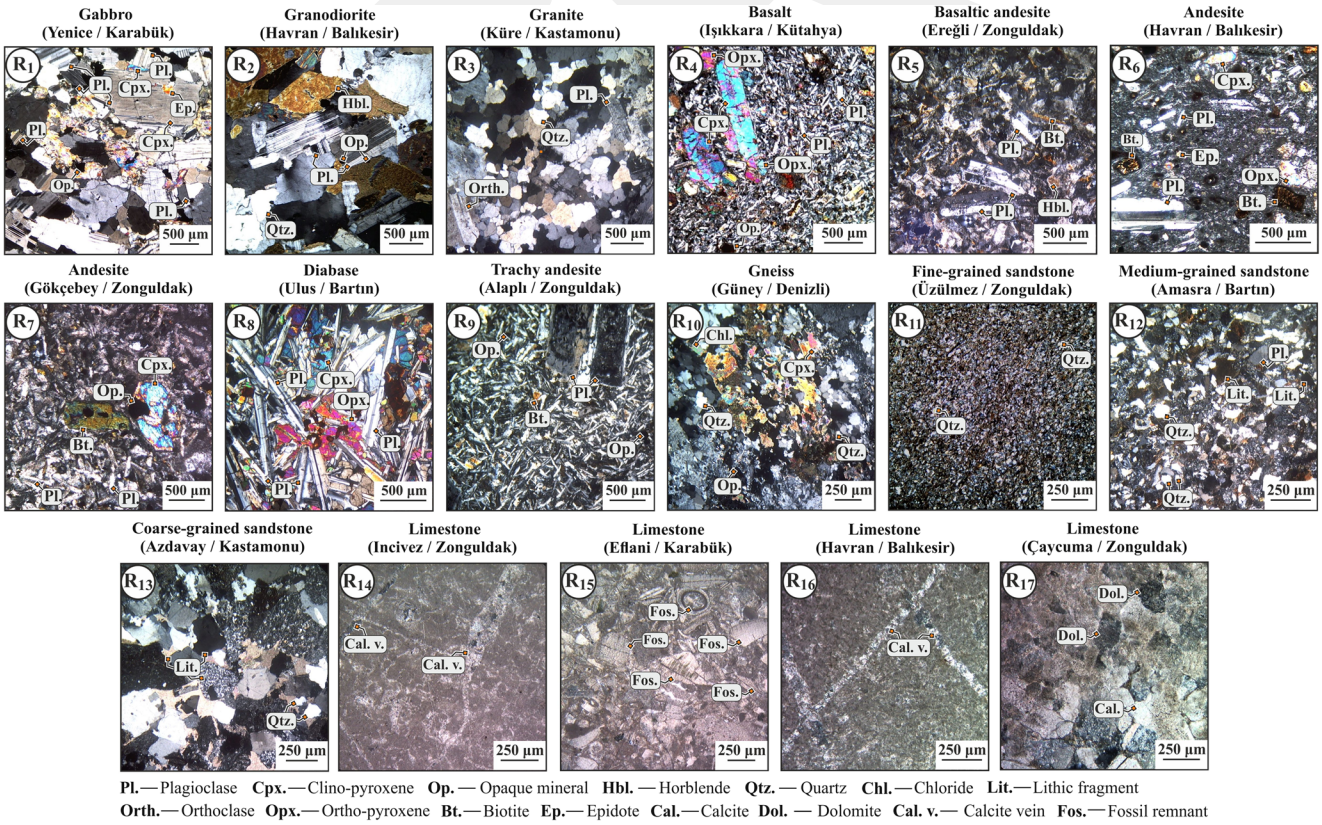

Fig. 2 Typical thin sections of the investigated rocks

Table 3 Mineralogical compositions (areal percentage) for each rock type

Minerals	Rock type																
	R_1	R_2	R_3	R_4	R_5	R_6	R_7	R_8	R_9	R_{10}	R_{11}	R_{12}	R_{13}	R_{14}	R_{15}	R_{16}	R_{17}
Quartz (%)	–	23	36	–	–	–	–	–		45	62	53	34	–	–	–	–
Orthoclase (K-feldspar, %)	–	10	15	–	–	–	–	–	11	12	–	–	–	–	–	–	–
Plagioclase (%)	62	40	29	46	64	52	75	65	44	16	3	5	2	–	–	–	–
Pyroxene (Opx + Cpx, %)	16	10	–	12	5		3	16	6	7	–	–	–	–	–	–	–
Olivine (%)	3	–	–	2	–		–	–			–	–	–	–	–	–	–
Hornblende (%)	4	5	7	10	20	5	1	8	15		–	–	–	–	–	–	–
Biotite (%)	2	8	5	6	–	10	3	5	1	7	–	–	–	–	–	–	–
Muscovite (%)	–	–	2	1	–		–	–	–	6	–	–	–	–	–	–	–
Epidote (%)	1	–	–	1	–	2	1	–			–	–	–	–	–	–	–
Chloride (%)	–	–	2	–	–		–	–		3	–	–	–	–	–	–	–
Calcite (microcrystalline + sparry, %)	–	–	–	–	–		–	–			–	–	–	90	74	85	80
Dolomite (%)	–	–	–	–	–		–	–			–	–	–	–	–	–	12
Opaque minerals (Hematite, magnetite, etc.) (%)	12	4	4	7	6	6	7	3	5	4	–	–	–	–	–	–	–
Lithic fragments (in sandstone, %)	–	–	–	–	–		–	–			35	42	64	–	–	–	–
Fossil remnant (skeletal and non-skeletal fragments in limestone, %)	–	–	–	–	–		–	–			–	–	–	10	26	15	8
Ground mass (matrix in igneous rocks, %)	–	–	–	15	5	25	10	3	18		–	–	–	–	–	–	–

composed of quartz and lithic fragments, and they were identified as lithic-arenite according to the sandstone classification of Folk (1981). A large number of soft calcite minerals comprise limestones ($R_{14–17}$), whose textures vary from mud-supported to crystalline type.

Physico-mechanical and aggregate properties of the rocks

The rock blocks obtained from the quarries were drilled, and cylindrical core samples with rough surfaces were obtained (Fig. 3a). The internal diameter of the core drill was 54.7 mm. The rough surface core samples were then cut and polished, regarding the geometrical instructions of related testing methods. The physical and mechanical properties of rocks were determined using these core samples in accordance with the suggested methods of ISRM (2007) under oven-dried conditions.

The physical properties of rocks considered in this study were dry density (ρ_d, g/cm^3) and water absorption by weight (w_a, %), where cylindrical core sample with a height to diameter ratio of 0.5–1.0 were used. The core samples were placed in a desiccator filled with distilled water for 24 h (Fig. 3b). A vacuum pump was used to reach an effective saturation of rock materials. Following the immersion of the core samples, the saturated mass of each core sample was measured. Then, the core samples were placed in a drying oven at 105 ± 2 °C for 24 h. After reaching to room temperature of the core samples, the oven-dried mass of each core sample was measured, and the physical properties of each core sample were determined considering the principles of soil mechanics based on the porosity-prism. During the determination of physical properties, five core samples were used, and the average value of each parameter was presented.

Shore hardness (SH) of rock materials was determined using a C − 2 type Shore scleroscope. A smooth-cut cylindrical core sample, whose volume was greater than 80 cm^3, was placed into the testing apparatus. The SH was determined by dropping the diamond-tipped hammer on the core sample, namely, recording rebounding heights of the diamond-tipped hammer (Fig. 3c). The SH tests were carried out at each surface (i.e., top and bottom surfaces) of the rock materials. A total of 20 measurements were recorded for each surface. The average value of rebounding heights of the diamond-tipped hammer was considered as the SH of the rock.

The BTS of rocks was determined using core samples with a height to diameter ratio of 0.5–1.0 (Fig. 3d), whereas the core samples with length to diameter ratio of 2.5–3.0 were used for the UCS tests (Fig. 3e). During the UCS and BTS tests, the stress rate of the stiff loading machine was within the limits of 0.5–1.0 MPa per second.

The mechanical aggregate properties of rocks considered in this study were the S_{20} brittleness index and the LAA.

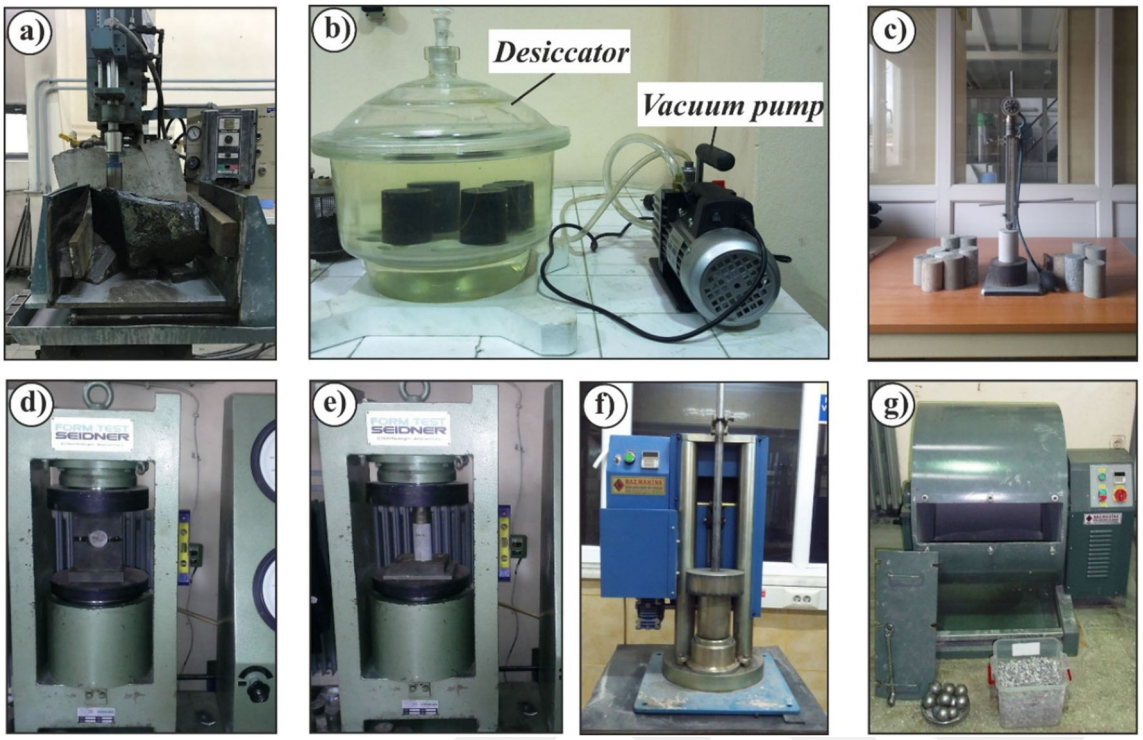

Fig. 3 Determination of physical, mechanical, and aggregate properties of rock materials. **a** Obtaining drill core samples. **b** Saturating of core samples. **c** C-2 type Shore scleroscope used in this study. **d** Brazilian tensile strength test. **e** Uniaxial compressive strength test. **f** S_{20} brittleness index test. **g** Los Angeles abrasion test

The S_{20} brittleness index test is suitable for aggregates with a particle size range of 11.2–16.0 mm. The initial mass of the sample (m_0) for the S_{20} brittleness index test was determined by the following equation:

$$m_0 = (500 \times \rho_d)/2.65 \quad (1)$$

where ρ_d is the dry density of the rock material (g/cm^3), and m_0 is in gram.

The rock aggregates with an initial mass of m_0 were placed in a cylindrical steel mold whose height and diameter was 75 mm and 125 mm, respectively. The rock aggregates were subjected to impact loads by a steel-hardened hammer that impacts a force of 137.34 N per drop from a specific height of 25 cm. The process was repeated for 20 times (Fig. 3f). Following that, the crushed particles were sieved through an 11.2-mm sieve, and the S_{20} brittleness index was determined by the following equation:

$$S_{20} = (m_1/m_0) \times 100 \quad (2)$$

where m_0 is the initial sample mass (g), and m_1 is the mass of crushed particles passing through the 11.2-mm sieve (g).

Los Angeles abrasion test gives a relative measure about fragmentation and abrasion resistance of rock aggregates. The LAA tests were carried out in accordance with TS EN 1097–2 (2010). A total amount of 5000 ± 5 g rock aggregates with a particle size range of 10–14 mm was prepared for each test. The rock aggregates together with 11 standardized steel spheres were placed in the LAA drum that horizontally rotates with 31–33 rpm. After 500 revolutions of the drum, the aggregates were obtained from the collecting vessel, and the LAA was determined by the following equation:

$$\mathrm{LAA} = ((m_2 - m_3)/m_2) \times 100 \quad (3)$$

where m_2 is the initial sample mass (g), and m_3 is the mass of crushed particles retained on the 1.6-mm sieve (g).

The laboratory test results are listed in Table 4. Accordingly, the UCS of the rocks approximately varies from 50 to 188 MPa. Considering these values, the investigated rocks were identified, varying from medium to very hard rocks, according to ISRM (2007). The brittleness degree of the rocks was found to be in a wide range (25–74%). According to the S_{20} classification of Dahl et al. (2012), most of the rocks have a degree of brittleness ranged from low to high.

Table 4 Physico-mechanical and aggregate properties of the investigated rocks

Rock type	ρ_d (g/cm^3)	w_a (%)	SH	UCS (MPa)	BTS (MPa)	S_{20} (%)	LAA (%)
R_1	2.88	0.11	86.7	188.29	20.25	25.41	14.66
R_2	2.77	0.28	73.6	154.34	7.50	33.88	25.26
R_3	2.68	0.40	60.8	75.90	8.21	56.70	30.51
R_4	2.74	0.32	76.2	143.66	15.47	36.52	15.40
R_5	2.68	0.74	66.4	118.15	9.11	49.60	20.46
R_6	2.38	1.55	39.5	84.54	5.91	40.32	35.17
R_7	2.36	2.35	56.5	106.56	6.24	39.66	26.86
R_8	2.76	0.20	89.4	163.82	18.25	29.14	12.91
R_9	2.53	1.40	62.5	71.10	9.20	56.30	26.85
R_{10}	2.64	0.44	53.4	80.96	7.55	54.83	29.53
R_{11}	2.60	1.48	62.5	144.47	11.20	30.51	21.36
R_{12}	2.58	3.95	52.2	73.23	6.25	69.60	35.22
R_{13}	2.59	6.83	35.4	49.70	2.11	74.20	44.14
R_{14}	2.63	0.45	37.7	70.30	6.08	56.10	30.68
R_{15}	2.57	0.78	41.1	64.64	4.36	65.90	31.48
R_{16}	2.59	0.30	44.7	82.32	7.56	46.24	21.80
R_{17}	2.60	0.45	49.5	108.62	8.68	39.01	24.29

ρ_d dry density, w_a water absorption by weight, *SH* Shore hardness, *UCS* uniaxial compressive strength, *BTS* Brazilian tensile strength, S_{20} the brittleness index, *LAA* Los Angeles abrasion loss

Crushability tests

The crushability tests are based on the fragmentation and comminution rate of rock aggregates occurred in a laboratory–scale cone crusher. The size and feeding mass of rock aggregates for the crushability tests were adopted from Dahl et al. (2012). In this context, rock aggregates with a particle size range of 11.2–16 mm were prepared for each rock type (Fig. 4a). The initial feeding mass (m_0) of the rock aggregates was determined by Eq. 1.

The implementation of the crushability tests is simple. The entire mass of aggregates (m_0) was fed to the cone crusher in a single charge by hand. The elapsed time throughout the crushing action (T_c, s) was recorded using a chronometer for each test. Before performing the crushability tests, the OSS and CSS of the cone crusher were adjusted as to 18 mm and 8 mm, respectively. The eccentric throw of the cone mantle was 10 mm. No further efforts were made about the calibration of the CSS since relatively low mass of feeding quantities ($m_0 = 445$–544 g) was charged to the crusher. During the crushability tests, the cone mantle eccentrically rotated with an average speed of 700 rpm at 50 Hz (Fig. 4b). Before and after each crushability test, uncrushed and crushed particles were sieved for the determination of their PSDs (Fig. 4c). Some of the crushed particles after crushability tests are shown in Fig. 4d–e.

The crushability tests were repeated five times for each rock type, and the DRC in cone crusher was quantified considering two simple approaches. One of them was based on the Taggart Method. The Taggart Method deals with feeding and product size fractions before and after crushability tests. Utilizing this method, the size reduction ratio (SRR) was determined for each rock type by the following equation:

$$\mathrm{SRR} = F_{80}/P_{80} \tag{4}$$

where F_{80} and P_{80} are the theoretical square mesh aperture sizes (mm) corresponding to the 80% of cumulative undersize in the feed and product, respectively.

The second approach to quantify the DRC was stated by investigating relatively finer product achievements in cone crushing. Herein, the DRC was assessed by determining the theoretical theoretical square mesh aperture size that corresponds to the %10 of cumulative undersize in the product (P_{10}, mm). The values of SRR and P_{10} were evaluated as a relative measure of the DRC in the cone crusher. The variations in several PSDs of the products are illustrated in Fig. 5 for several rock types.

The crushability test results are given in Table 5. Accordingly, the SRR of the investigated rocks was found to be in the range of 2.69–3.52. The P_{10} was obtained, ranging from 0.43–1.44 mm. The T_c was also between 11.4 and 29.4 s for the investigated rocks.

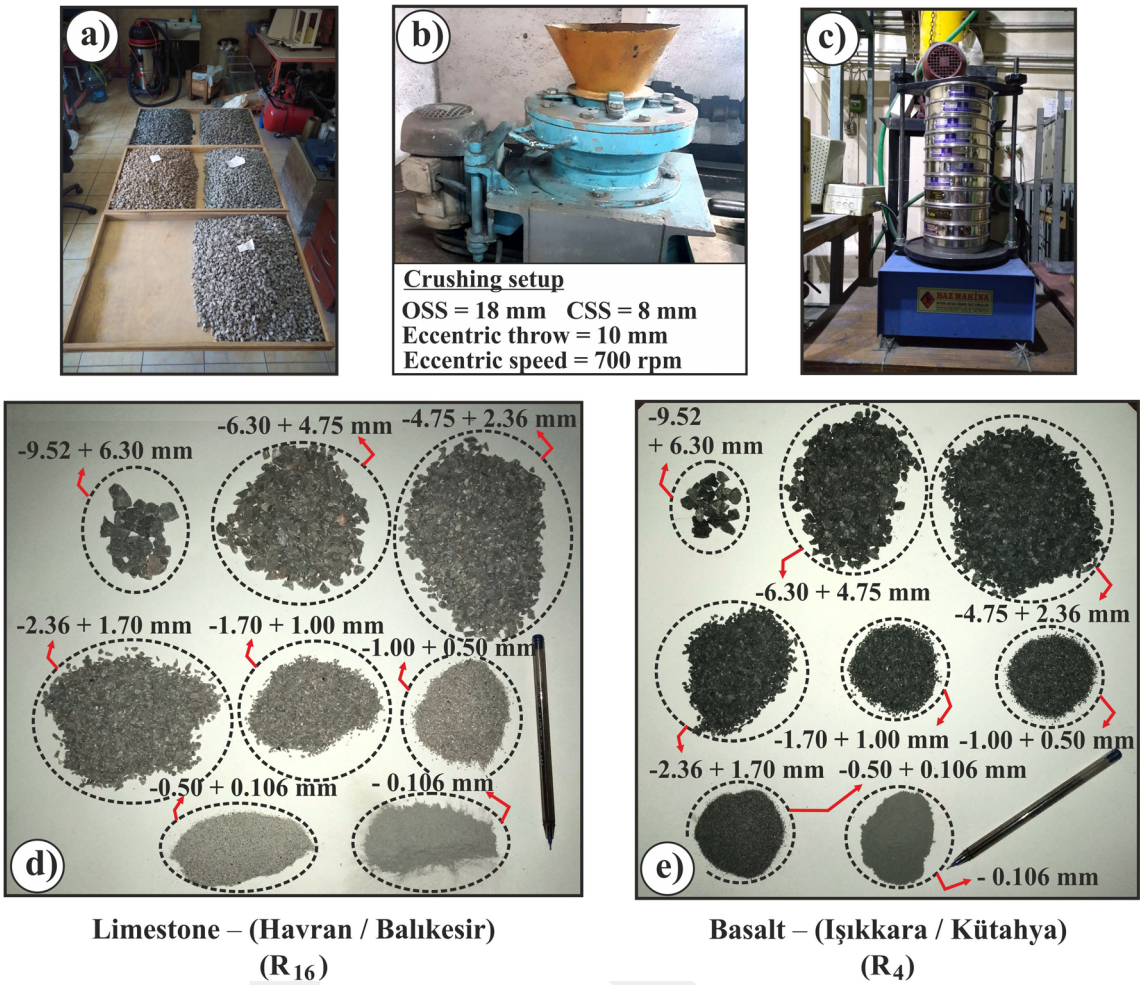

Fig. 4 Laboratory equipment used and materials studied in the crushability tests. **a** Some of the prepared crushed rock aggregates with a particle size range of 11.2–16 mm. **b** Laboratory-scale cone crusher used in this study. **c** Sieve shaker and sieves used in this study. **d** Crushed particles for R_{16}. **e** Crushed particles for R_4

Results and discussion

The variations in SRR, T_c, and P_{10} due to rock properties

When comparing the rock properties (Table 4) with the SRR values, it was determined that there is a close relationship between the SRR, LAA, and BTS of the rocks. From this point of view, higher SRR values indicate lower crushing resistance of rock aggregates so that the variations in SRR values could reflect the DRC for specific crushing operations from engineering geological aspects. On the other hand, the P_{10} is highly dependent upon the SH. Moreover, the BTS also seems to have an influence on the P_{10} (Table 6).

The variations in the P_{10} could be evaluated in fine crushing resistance of the rocks, which could be attributed to the fact that a lower value of P_{10} represents a greater amount of finer product achievement in cone crushing or vice versa.

The progressive size-reduction event in cone crusher is a complex phenomenon. It seems that, during the crushing action in cone crusher, rock aggregates are broken down due to exceeding the BTS of rocks. Finer materials are generated by abrasion, smashing of crushed particles between cone mantle and concave chamber as well as the inter-particle compression. Thus, the fine crushing event in cone crusher is gradually accomplished under the combined effects of mineral hardness and micro-strength of crushed particles. However, the shape and size fraction of the products are changeable in terms of various rock lithologies.

For very strong igneous rocks (R_1, R_2, R_4, and R_8), the crushed particles retained on a 6.3-mm sieve were mainly observed as elongated products, whereas the ones passing through a 4.75-mm sieve were almost identical and cubical. For the andesitic rocks ($R_{5–7}$, R_9), the number of crushed particles with − 4.75 + 2.36 mm increased considerably compared with those mentioned herein.

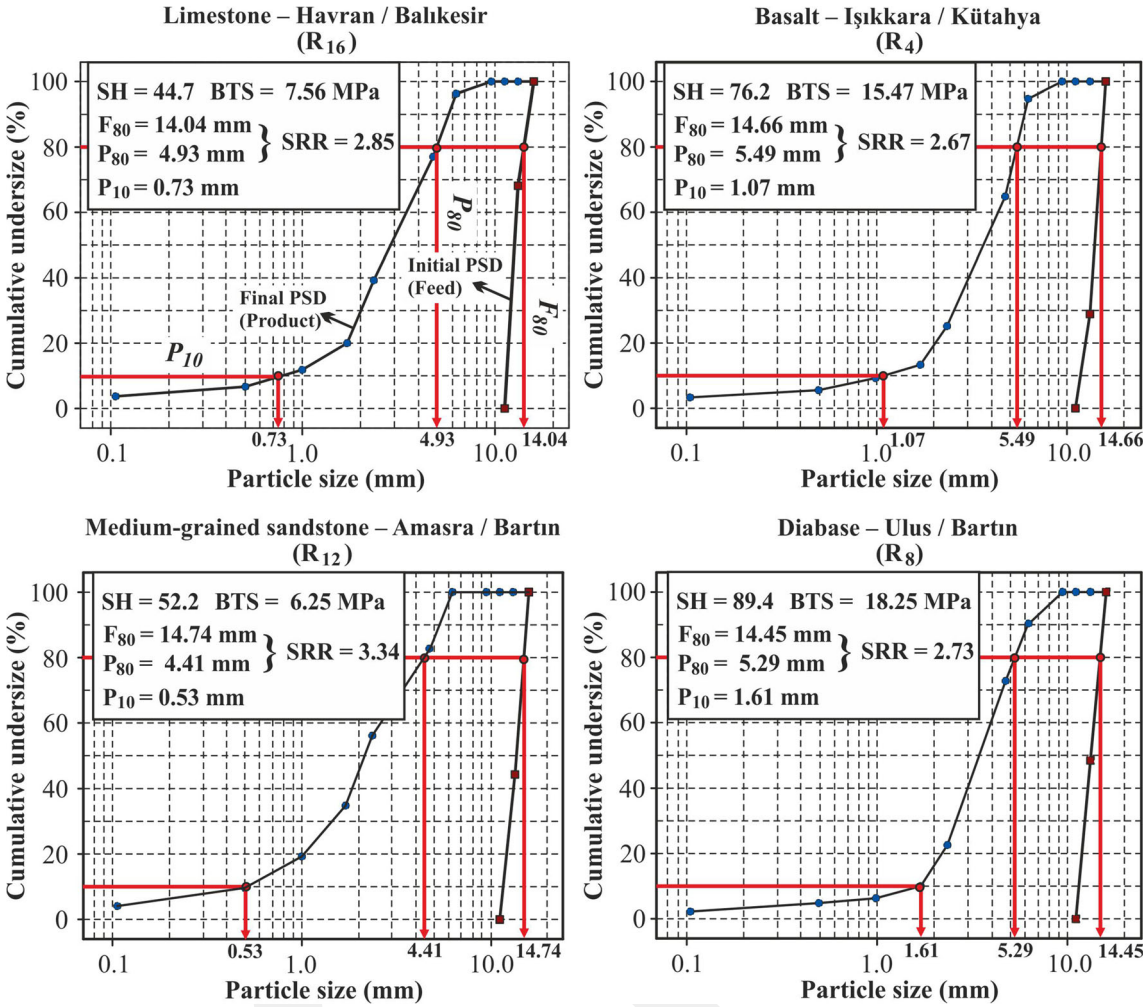

Fig. 5 Typical final PSDs of the products obtained from several crushability tests

Table 5 Crushability test results

Rock type	F_{80} (mm)	P_{80} (mm)	P_{10} (mm)	SRR	Crushing time, T_c (s)
R_1	15.21	5.59	1.25	2.72	28.3
R_2	13.43	4.33	1.04	3.10	20.7
R_3	15.06	5.04	0.92	2.99	17.4
R_4	14.52	5.39	1.07	2.69	29.1
R_5	14.03	4.89	0.81	2.87	20.6
R_6	14.92	4.36	0.49	3.42	15.7
R_7	13.85	4.17	0.76	3.32	18.5
R_8	14.31	5.28	1.44	2.71	29.4
R_9	14.87	4.73	0.94	3.14	18.7
R_{10}	14.28	4.43	0.88	3.22	17.2
R_{11}	13.57	4.76	0.81	2.85	17.7
R_{12}	14.59	4.62	0.56	3.37	15.5
R_{13}	13.97	3.97	0.43	3.52	11.4
R_{14}	14.50	4.57	0.66	3.17	16.8
R_{15}	14.03	4.20	0.63	3.34	18.4
R_{16}	14.66	4.75	0.70	3.09	17.3
R_{17}	14.24	5.01	0.85	2.84	16.7

Table 6 Pearson's correlation matrix for the variables considered in this study

Parameter	ρ_d (g/cm^3)	w_a (%)	SH	UCS (MPa)	BTS (MPa)	S_{20} (%)	LAA (%)	SRR	P_{10} (mm)	T_c (s)
ρ_d (g/cm^3)	1									
w_a (%)	− 0.385	1								
SH	0.680	− 0.447	1							
UCS (MPa)	0.619	− 0.472	0.870	1						
BTS (MPa)	0.666	− 0.515	0.881	0.847	1					
S_{20} (%)	− 0.322	0.593	− 0.680	− 0.890	− 0.737	1				
LAA (%)	− 0.561	0.711	− 0.815	− 0.834	− 0.876	0.801	1			
SRR	− 0.688	0.646	− 0.779	− 0.782	**− 0.863**	0.711	**0.909**	1		
P_{10} (mm)	0.700	− 0.609	**0.926**	0.795	**0.878**	− 0.684	− 0.838	− 0.813	1	
T_c (s)	0.645	− 0.569	**0.879**	0.816	**0.911**	− 0.676	**− 0.872**	− 0.782	0.876	1

* Bolded values (e.g., **0.911**) indicate the most important variables affecting the SRR, P_{10}, and T_c

For the sandstones ($R_{11–13}$), the cumulative quantity of 50–70% of the products was obtained in the particle size range of + 1.70–4.75 mm. They were almost well rounded and mostly identical in shape for medium and coarse-grained sandstones ($R_{12–13}$). However, plenty of products retained on a 4.75-mm sieve were elongated for fine-grained sandstones (R_{11}). Rock comminution in the limestones ($R_{14–17}$) occurred as a brittle failure. The products retained on a 2.36-mm sieve were still elongated for mud-supported limestones ($R_{14–16}$). In contrast, they were almost cubical and identical in shape for crystalline limestones (R_{17}).

The variations in the SRR and P_{10} values due to several rock properties are given in Fig. 6. As seen in the figure, the SRR varied from 2.69–3.52. In general, the DRC increases in parallel with the LAA of rocks. However, it decreases with increasing the BTS of rocks (Fig. 6a). The P_{10} was found to be in the range of 0.43–1.44 mm. Finer product achievement increases with decreasing the BTS and SH of rocks (Fig. 6b).

It was also determined that the T_c increases with increasing SH, BTS, but decreasing the LAA of rocks (Table 5). Increasing the T_c during any crushing operation could be linked to higher energy consumption that can be revealed as a function of the BTS (Eq. 5) in this study. Briefly, increasing rock strength, especially the BTS of rocks, could be considered for estimating the energy consumption in cone crushing. Although the crusher types are different, the background of Eq. 5 supposes the findings of Olaleye (2010) conceptually. In addition, increasing the BTS of rock inevitably causes a

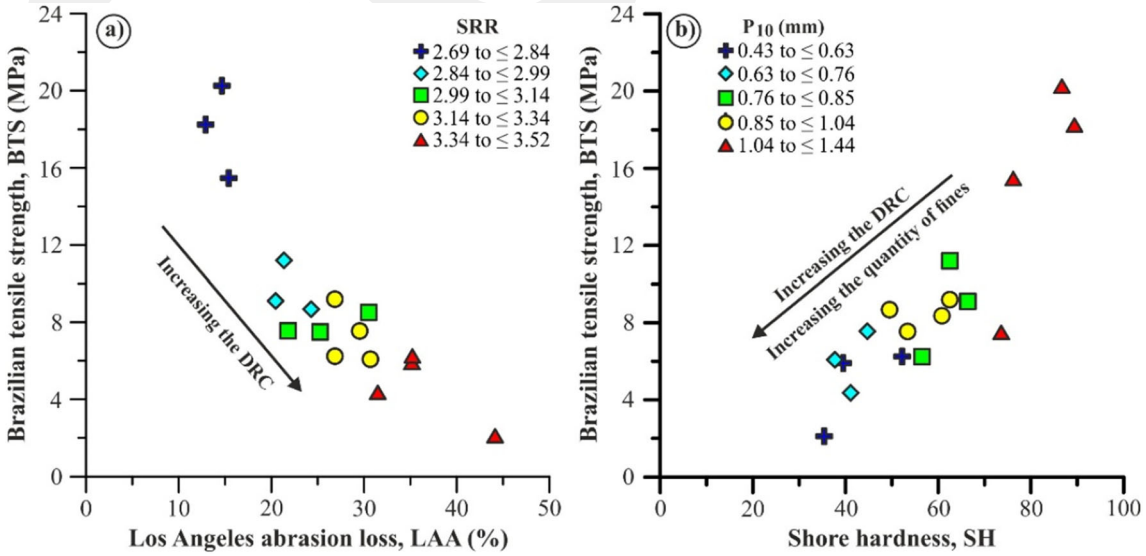

Fig. 6 The variations in the DRC due to several rock properties. **a** The SRR. **b** The P_{10}

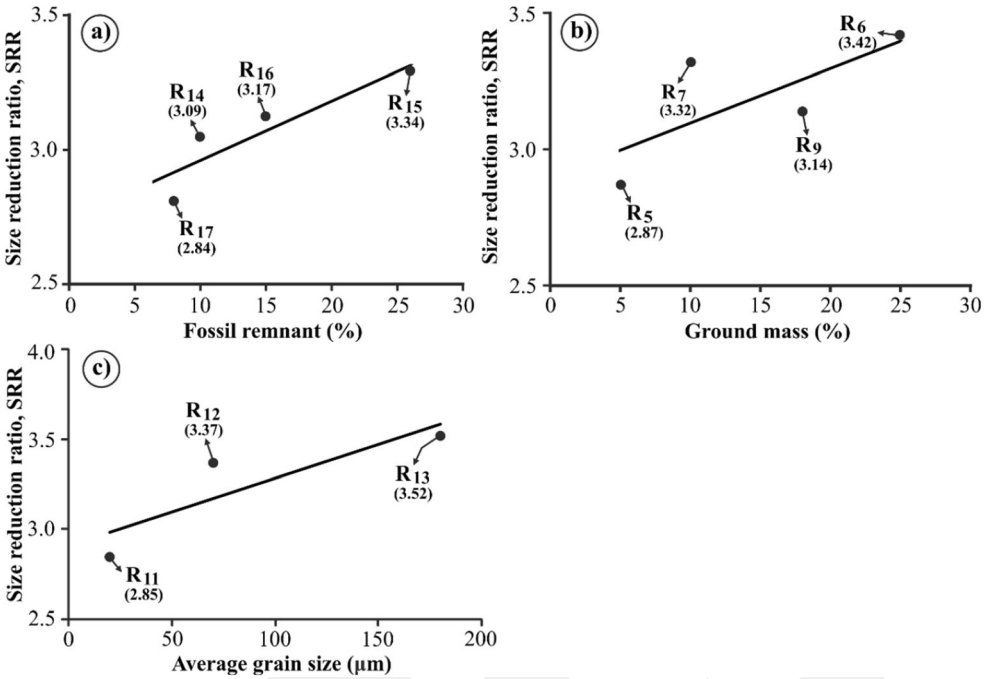

Fig. 7 Textural and mineralogical effects on the SRR for several rock types. **a** Effects of fossil remnant for limestones. **b** Effects of groundmass for andesites. **c** Effects of average grain size for sandstones

higher degree of wear in cone mantle liners. However, the wear degree of cone mantle was not considered in this study.

$$T_c = 10.76 + 0.95BTS, R^2 = 0.77 \quad (5)$$

In general, one could claim that the above-mentioned variables (SRR, P_{10}, and T_c) are mainly associated with the BTS, LAA, and SH of rocks. In this regard, these variables could provide satisfactory knowledge and enable rapid estimations about the rock comminution in cone crushing from different aspects.

The variations in SRR due to textural and mineralogical properties of rocks

Based on the petrological variances of the rocks, the mafic rocks (R_1, R_4, and R_8) seemed to have a greater crushing resistance compared with the felsic rocks ($R_{2–3}$). The textural and mineralogical properties of rocks also influenced the SRR.

For the limestones ($R_{14–17}$), the SRR increased in parallel with the number of fossil remnants (Fig. 7a). However, the variations in the fossil type had no significant effects on the SRR. Focusing on the textural properties of the andesitic rocks, the variations in the textural properties of andesites seemed not to affect the SRR. However, increasing the quantity of groundmass led to an increase in the SRR (Fig. 7b). In addition, higher SRR values were obtained for several andesitic rocks (R_6) that bear higher amounts of weathered rock-forming minerals such as plagioclase, hornblende, and biotite.

The attrition typology of rock aggregates was transformed from fragmentation to chipping as the grain size increases in the sandstones ($R_{11–13}$). In addition, the SRR increased with an increasing average grain size. It can be claimed that the rock comminution in cone crushing could be relatively easier for handling sandstones with coarser grain sizes (Fig. 7c).

The effects of grain size on the strength properties of the sandstones could also be observed when focusing on the strength properties of the sandstones (Table 3). Accordingly, the UCS and BTS of sandstones decrease with increasing the average grain size. This finding is also in a good agreement with the findings of several researchers (Hugman and Friedman 1979; Wong et al. 1996; Eberhardt et al. 1999; Tugrul and Zarif 1999; Přikryl 2001; Cai et al. 2004; Nicksiar and Martin 2014; Köken 2020).

Further research potentials on the DRC in cone crusher

The quantification of DRC in cone crusher could be revealed by the SRR and P_{10}. In this context, the performance of cone crushing operations could be explored considering the variations in SRR, where higher values of SRR could point out the relative success of crushing operations. However, the SRR itself is not sufficient for the evaluation of the DRC in cone crusher. The fine product achievement or minimization of fines during cone

crushing could be easily revealed by focusing on the P_{10}. Therefore, the SRR and P_{10} should be considered together for optimum rock comminution in cone crushing. However, further efforts are still needed to combine these variables with product flakiness and production yield for specific size fractions. Based on the experiences on the crushability tests and given variations in the SRR and P_{10} due to different rock lithologies (Table 4) could encourage researchers to investigate the performance of crushing operations either of a single rock type or interrelated rock mixtures (e.g., andesites-basaltic andesites, or limestone mixtures, etc.) by changing operational factors such as the CSS, eccentric speed, or feeding size fractions.

The choke feeding method was employed manually in this study, and the T_c was measured in this direction. Automated systems for choke feeding could also be a great contribution to such DRC studies in cone crushers. The effects of feed rate concerning both production yield, product flakiness, and energy consumption could be regarded by vibrating or non-vibrating feeders that enable researchers to investigate the intensity of choke feeding during cone crushing.

The textural and mineralogical properties have several influences on the DRC for several rock types (Fig. 7). From this point of view, the variations in the SRR and P_{10} values could be taken part in evaluating the weathering degree of rocks. Providing that all operational factors are to be fixed in cone crushing, it is probably expected that the SRR of rocks would change owing to mineralogical and textural variances induced by rock weathering processes. Similarly, should the P_{10} be considered, it would also be a beneficial parameter to distinguish the structural zones in/on rock masses, where drilling and blasting operations are performed.

Minimizing fine and flaky materials in conjunction with optimum energy consumption is of prime importance for rock quarrying (Briggs and Evertsson 1998; Mitchell et al. 2008; Major 2009; Wills and Finch 2015; Lynch 2015; Gupta and Yan 2016). In this study, it was achieved that the T_c could be correlated with the BTS, LAA, and SH of rocks (Table 5). Therefore, these variables, one of which (BTS, MPa) was indirectly emphasized by Bearman et al. (1997), might be beneficial for the evaluation of crushing energy consumption. To illustrate the effects of rock strength on the DRC, the Eq. 5 was derived. In this concept, such empirical relationships like Eq. 5 should be further explored for specific crushing operations that provide benefits for rock aggregate manufacturers in terms of the crushing energy optimizations.

Based on product flakiness, it was previously mentioned that plenty of the products retained on various sieves (e.g., the 6.3-mm sieve for R_1, R_2, R_4, R_8; the 4.75-mm sieve for R_{11}, and the 2.36-mm sieve for $R_{14–16}$) were flaky. In addition to Eloranta (1995), the minimization of flaky products and attempts on increasing production yield for specific size fractions should also be further investigated by changing the quantity of feed that could have a direct link to the intensity of choke feeding, whereby discontinuous feeding methods could even be attempted for rocks with medium (UCS = 50–100 MPa) and weak strength (UCS < 50 MPa).

Conclusions

The DRC in cone crusher was investigated using a laboratory-scale cone crusher. A total of 17 rock types were characterized by mineralogical analyses, and several physico-mechanical and aggregate properties were determined for each rock type. The present study states the geological-based factors on the DRC in cone crusher to some extent, and the main conclusions could be drawn as follows:

- The DRC in cone crusher could be quantified using the SRR and P_{10}. These variables are dependent upon the BTS, LAA, and SH rocks (Fig. 6). Textural and mineralogical features also have influences on the DRC for several rock types (Fig. 7). Moreover, the T_c as a relative sign of crushing energy consumption could also be correlated with the BTS, LAA, or SH of rocks (e.g., Eq. 5).
- Considering the SRR and P_{10} together, the design, optimization, or routine control of secondary and tertiary cone crushing operations could be carried out more accurately. These variables could also be utilized in evaluating rock weathering processes that directly affect the quality of rock aggregates. However, further efforts are required in this regard.
- The SRR seems to increase with:

  – increasing the quantity of groundmass for andesitic rocks.
  – increasing the quantity of fossil remnants for limestones.
  – increasing the average grain size for sandstones.

- To minimize fine and flaky products in cone crushing, several variables should be considered for further DRC studies as follows:

  – Rock lithology and weathering.
  – Rock aggregate size and initial PSD of feed.
  – Feed rate changeable with vibrating or non-vibrating feeders.
  – CSS and eccentric speed of cone crusher.
  – Wear condition of cone crusher.

Last but not least, the quantitative approaches stated in this study should be attempted to such industrial crushing—screening plants operated with cone crushers to observe difficulties/similarities of quantifying the DRC. Direct measurements of crushing energy consumption in cone crushers

could also be beneficial to achieve a comprehensive understanding of how effective the BTS would be in cone crushing.

Acknowledgments The author is greatly indebted to Dr. Raşit Altındağ (Süleyman Demirel University, Turkey) and Dr. Ahmet Özarslan (Zonguldak Bülent Ecevit University, Turkey) for providing laboratory facilities and their help during laboratory studies. The author also appreciates the constructive comments and suggestions of the anonymous reviewers that improved the manuscript.

References

Bearman RA, Briggs CA, Kojovic T (1997) The application of rock mechanics parameters to the prediction of comminution behavior. Miner Eng 10(3):255–264. https://doi.org/10.1016/S0892-6875(97)00002-2

Bengtsson M. and Evertsson C.M. (2006) An empirical model for predicting flakiness in cone crushing, Int. J Miner Process 79(1): 49–60, https://doi.org/10.1016/j.minpro.2005.12.002

Briggs C, Evertsson CM (1998) Shape potential of rock. Miner Eng 11(2):125–132. https://doi.org/10.1016/S0892-6875(97)00145-3

Cai M, Kaiser PK, Tasaka Y, Maejima T, Morioka H, Minami M (2004) Generalized crack initiation and crack damage stress thresholds of brittle rock masses near underground excavations. Int J Rock Mech Min Sci 41:833–847. https://doi.org/10.1016/j.ijrmms.2004.02.001

Comakli R, Cayirli S (2019) A correlative study on textural properties and crushability of rocks. Bull Eng Geol Environ 78:3541–3557. https://doi.org/10.1007/s10064-018-1357-8

Dahl F, Bruland A, Jakobsen PD, Nilsen B, Grov E (2012) Classifications of properties influencing the drillability of rocks based on NTNU/SINTEF test method. Tunneling and Underground Space Technol 28:150–158. https://doi.org/10.1016/j.tust.2011.10.006

Donovan J. G. (2003) Fracture toughness based models for the prediction of power consumption, product size, and capacity of jaw crushers, Dissertation, Virginia Polytechnic Institute, and State University, 211 pp.

Eberhardt E., Stimson B. and Stead D. (1999) Effects of grain size on the initiation and propagation thresholds of stress-induced brittle fractures, Rock Mech. Rock Eng 32(2) 81–99, https://doi.org/10.1007/s006030050026

Eloranta J. (1995) Influence of crushing process variables on the product quality of crushed rock, Dissertation, Tampere University of Technology, pp 118

Evertsson CM (1998) Output prediction of cone crushers. Miner Eng 11(3):215–231. https://doi.org/10.1016/S0892-6875(98)00001-6

Folk R.L. (1981) Petrology of sedimentary rocks, Hemphill publishing, 190 pp, Austin

Gent M, Menendez M, Torano J, Torno S (2012) A correlation between Vickers hardness indentation values and the Bond Work Index for the grinding of brittle minerals. Powder Technol 224:217–222. https://doi.org/10.1016/j.powtec.2012.02.056

Guimaraes MS, Valdes JR, Palomino AM, Santamarina JC (2007) Aggregate production: fines generation during rock crushing. Int J Miner Process 81(4):237–247. https://doi.org/10.1016/j.minpro.2006.08.004

Gupta A. and Yan D. (2016) Mineral processing, 1 design, and operations: an introduction, Second Edition, Elsevier Press, Cambridge 856 pp.

Heikkila P. (1991) Improving the quality of crushed rock aggregate, Dissertation, Helsinki University of Technology, pp 191

Hugman RHH, Friedman M (1979) Effects of texture and composition on mechanical behavior of experimentally deformed carbonate rocks. AAPG Bull 63(9):1478–1489. https://doi.org/10.1306/2F9185C7-16CE-11D7-8645000102C1865D

ISRM (2007) The complete ISRM suggested methods for rock characterization, testing and monitoring, 1974–2006, In: Ulusay R, Hudson J.A. (Eds), Int. Soc. Rock. Mech. (ISRM) Ankara, Turkey

Kahraman S, Toraman OY (2008) Predicting Los Angeles abrasion loss of rock aggregates from crushability index. Bull Mater Sci 31(2): 173–177. https://doi.org/10.1007/s12034-008-0030-4

Kahraman S, Toraman OY, Cayirli S (2018) Predicting the strength and brittleness of rocks from a crushability index. Bull Eng Geol Environ 77(4):1639–1645. https://doi.org/10.1007/s10064-017-1012-9

Kekec B, Unal M, Sensogut C (2006) Effect of textural properties of rocks on their crushing and grinding features. J Univ Sci Technol Beijing 13(5):385–392. https://doi.org/10.1016/S1005-8850(06)60079-0

Kelly EG, Spottiswood DJ (1982) Introduction to mineral processing. John Wiley, Newyork, p 491

Köken E (2020) Investigations on fracture evolution of coal measure sandstones from mineralogical and textural points of view. Indian Geotech J. https://doi.org/10.1007/s40098-020-00427-1

Köken E, Özarslan A (2018) New testing methodology for the quantification of rock crushability: compressive crushing value (CCV). Int J Miner Metall Mater 25(11):1227–1236. https://doi.org/10.1007/s12613-018-1675-7

Korman T, Bedekovic G, Kujundzic T, Kuhinek D (2015) Impact of physical and mechanical properties of rocks on energy consumption of jaw crusher. Physicochem Probl Miner Process 51(2):461–475. https://doi.org/10.5277/ppmp150208

Lee E, Evertsson CM (2011) A comparative study between cone crushers and theoretically optimal crushing sequences. Miner Eng 24:188–194. https://doi.org/10.1016/j.mineng.2010.07.013

Lynch A. (2015) Comminution handbook – Spectrum 21, The Australasian Institute of Mining and Metallurgy, ISBN: 978-1-925100-38-9, 340 pp,

Ma Y, Fan X, He Q (2016) Prediction of cone crusher performance considering liner wear. Appl Sci 6(12):404. https://doi.org/10.3390/app6120404

Major, K. (2009) Factors influencing the selection and sizing of crushers. In: Malhotra, D. et al., (Eds.), Recent advances in mineral processing plant design. SME, Englewood, USA, 356–360

Mitchell C.J, Mitchell P. and Pascoe R.D. (2008) Quarry fines minimization: can we really have 10 mm aggregates with no fines? Proceedings of the 14th Extractive Industry Geology Conference, Scott P.W. and Walton G. (Eds), 37–44, http://nora.nerc.ac.uk/id/eprint/4932

Mwanga A, Rosenkranz J, Lamberg P (2015) Testing of ore comminution behavior in the geometallurgical context – a review. Minerals 5(2):276–297. https://doi.org/10.3390/min5020276

Nicksiar M, Martin CD (2014) Factors affecting crack initiation in low porosity crystalline rocks. Rock Mech Rock Eng 47:1165–1181. https://doi.org/10.1007/s00603-013-0451-2

Olaleye BM (2010) Influence of some rock strength properties on jaw crusher performance in granite quarry. Min Sci Technol (China) 20(2):208–208. https://doi.org/10.1016/S1674-5264(09)60185-X

Öztürk CA, Nasuf E, Bilgin N (2004) The assessment of rock cutability and physical and mechanical properties from a texture coefficient. J South Arf Inst Min Metall 104(7):397–402

Přikryl R (2001) Some microstructural aspects of strength variation in rocks. Int J Rock Mech Min Sci 38(5):671–682. https://doi.org/10.1016/S1365-1609(01)00031-4

Quist J, Evertsson CM (2016) Cone crusher modeling and simulation using DEM. Miner Eng 85:92–105. https://doi.org/10.1016/j.mineng.2015.11.004

Terva J, Kuokkala VT, Valtonen K, Siitonen P (2018) Effects of compression and sliding on the wear and energy consumption in mineral

crushing. Wear 398–399:116–126. https://doi.org/10.1016/j.wear.2017.12.004

Toraman OY, Kahraman S, Cayirli S (2010) Predicting the crushability of rocks from the impact strength index. Min Eng 23:752–754. https://doi.org/10.1016/j.mineng.2010.04.004

TS EN 1097–2 (2010) Tests for mechanical and physical properties of aggregates – part 2: methods for the determination of resistance to fragmentation, 36 pp.

Tugrul A, Zarif IH (1999) Correlation of mineralogical and textural characteristics with engineering properties of selected granitic rocks from Turkey. Eng Geol 51:303–317. https://doi.org/10.1016/S0013-7952(98)00071-4

Wills, B. A., Finch, J. A. (2015) Wills' mineral processing technology: an introduction to the practical aspects of ore treatment and mineral recovery, Butterworth-Heinemann

Wong RHC, Chau KT, Wang P (1996) Microcracking and grain size effect in Yuen Long marbles. Int J Rock Mech Min Sci Geomech Abstr 33(5):479–485. https://doi.org/10.1016/0148-9062(96)00007-1

Yılmaz NG (2011) Abrasivity assessment of granitic building stones in relation to diamond tool wear rate using mineralogy-based rock hardness indexes. Rock Mech Rock Eng 44:725–733. https://doi.org/10.1007/s00603-011-0166-1

Zeng Y, Forssberg E (1992) Energy consumption in fine crushing and dry rod grinding. Min Metall Explor 9(2):69–72